TECHNICAL ARTICLE

Observation of multiple Bragg reflections accompanying forbidden Si(002) reflection in bent-perfect Si crystal

P. Mikula [a], M. Vrána, J. Šaroun, and V. Ryukhtin
Nuclear Physics Institute of the Czech Academy of Sciences, Husinec – Řež 130, 250 68 Řež, Czech Republic

(Received 2 October 2020; accepted 14 December 2020)

Strong multiple Bragg reflections (MBRs) which can be realized in a bent-perfect-crystal (BPC) slab provide a monochromatic beam of excellent resolution parameters. For identifying MBR effects in the BPC Si crystal, we used the method of azimuthal rotation of the crystal lattice around the scattering vector of the primary forbidden Si(200) reflection for a fixed chosen wavelength. In this paper, several azimuthal scans searching strong MBR effects with the intention of a possible practical exploitation for very high-resolution diffractometry are presented. © *The Author(s), 2021. Published by Cambridge University Press on behalf of International Centre for Diffraction Data.*
[doi:10.1017/S0885715620000779]

Key words: neutron diffraction, multiple reflections, bent-perfect crystal, Bragg diffraction optics

I. INTRODUCTION

Even though the neutron sources provide currents several orders of magnitude lower than X-ray sources, there is a permanent attention paid to find the ways or methods and techniques helping in increasing the luminosity, and/or resolution of neutron scattering instruments. In addition to construction of high-flux neutron sources, a broad range of efficient neutron techniques, namely based on Bragg diffraction optics, have been recently developed (see, e.g., Popovici and Yelon, 1994, 1995; Vogt *et al.*, 1994; Mikula *et al.,* 2008a, 2014c; Mikula and Vrána, 2015; Seong *et al.*, 2010). This effort is strengthened not only by a necessity of investigations of samples of smaller dimensions but also by a necessity of using significantly better measurement resolution for investigation of finer effects, e.g., distinguishing and identifying powder diffraction lines corresponding to very close values of lattice spacings, for studies of plastic deformation by means of diffraction profile analysis and for studies of mosaic distribution of mosaic single crystals. Namely, the latter one requires a substantial increase of angular and/or energy resolution of conventional diffractometers/spectrometers operating, where the monochromator plays a key role. Bent-perfect-crystal (BPC) slabs as an excellent alternative of conventional mosaic crystals provide a way to increase luminosity and/or angular/energy resolution of some scattering devices installed at steady-state sources (Popovici and Yelon, 1995). An increase of the luminosity is carried out by focusing in real space, while a higher resolution can be achieved by focusing in momentum space in combination with a rather small effective mosaicity of the bent-perfect crystals. In this way, excellent results have been achieved in powder diffractometry and, namely, in the case of the residual stress diffractometer where by using the BPC monochromator the figure of merit of the instrument increased by a factor of 10 or more (Popovici and Yelon, 1994; Vogt *et al.*, 1994; Mikula *et al.*, 1996; Wimpory *et al.*, 2008; Seong *et al.*, 2010; Woo *et al.*, 2011). Together with the construction of new powerful neutron sources, designs of new scattering instruments with improved resolution properties are required. In this way, the so-called dispersive monochromators based on a dispersive double-diffraction process appear as candidates of monochromators for (very) high-resolution neutron diffractometers and spectrometers. It can be realized either by means of two independent crystals (Mikula *et al.*, 2014a, 2014b, 2014c; Mikula and Vrána, 2015) or by means of strong multiple Bragg reflections (MBRs) realized inside one crystal (Mikula *et al.*, 2006a, 2008a, 2011a, 2013). First, high-resolution MBR monochromators have been tested using neutron radiography for investigation of edge refraction effects (Mikula *et al.*, 2008b, 2013).

MBR effects are well known in X-ray diffraction when the positive MBR-diffraction peaks were first observed by Renninger (Renninger, 1937, 1960). Many other related references can be found, e.g., in the books of Pinsker and Chang (Pinsker, 1982; Chang, 1984). Concerning neutrons, relatively small MBR effects were observed in mosaic crystals (Moon and Shull, 1964; Kuich and Rauch, 1965, 1967). However, only in the case of elastically deformed BPC slabs have very strong MBR effects consisting in one or more double-diffraction processes been observed. Elastic deformation can strongly amplify the MBR effects and their related intensities can be more than one order of magnitude higher than the intensity related to the allowed reflection of a perfect nondeformed crystal (Mikula *et al.*, 2008b, 2011a, 2011b, 2012). In the last decade, we have paid systematic attention to studying these effects, namely when it has been found that some strong MBR effects can be considered as alternative to very high-resolution dispersive double-crystal neutron monochromators (Popovici and Yelon, 1995; Mikula *et al.*, 2014; Mikula and Vrána, 2015). As the MBR is, in fact, the dispersive double-diffraction process realized in one elastically deformed crystal, the aim of the present studies is a further search of strong MBR effects (in this case in relation to the forbidden Si(002) reflection at the constant neutron wavelength of 0.162 nm) which could potentially be an alternative to the

[a]Author to whom correspondence should be addressed. Electronic mail: mikula@ujf.cas.cz

 0885-7156/2021/36(1)/14/6/$18.00

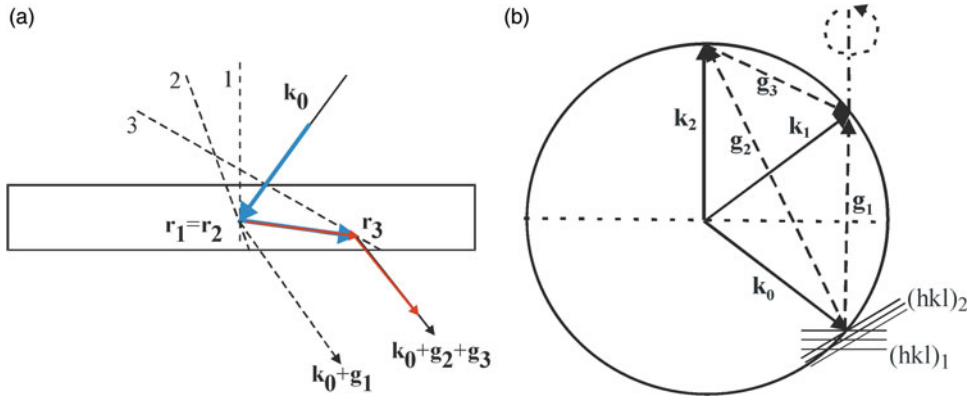

Figure 1. Schematic diagram of a two-step MBR simulating a primary reflection in real (a) and reciprocal space (b) for two reciprocal lattice points on the Ewald sphere. The numbers 1, 2, and 3 represent the primary, secondary, and tertiary reflection planes, respectively.

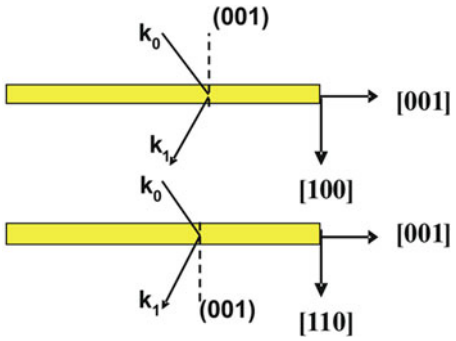

Figure 2. Top view on two crystal cuts of the Si slabs that were used in the experimental search of MBR effects in symmetric transmission geometry.

standard dispersive double-crystal monochromator (Popovici and Yelon, 1995; Mikula and Vrána, 2015).

II. SEARCH FOR MBR EFFECTS

It is known that the MBR effects in a single crystal can be observed when more than one set of planes are simultaneously operative for a given wavelength, i.e., when two or more reciprocal lattice points are on the Ewald sphere (see Figure 1). In the search of them, two methods are usually used:

- The method of $\theta-2\theta$ scan (related usually to weak or forbidden reflection) in the white beam for a fixed azimuthal angle, which is in fact based on changing the radius of the Ewald sphere (see, e.g., Mikula *et al.*, 2006b, 2008b).
- The method of azimuthal rotation of the crystal lattice around the scattering vector of the primary reflection for a fixed wavelength [see Figure 1(b)].

For the experimental studies of MBR effects, two Si slabs of different crystal cuts were chosen (see Figure 2). During the experiment, in both cases the bent Si slabs were set for diffraction on (002) planes in symmetric transmission geometry at the mean Bragg angle $\theta = 17.4°$ (for $\lambda = 0.162$ nm). The dimensions of the slabs were $200 \times 40 \times 3.5$ mm^3 (length × height × thickness). The thickness of 3.5 mm permitted us to bend the slabs in a rather large range of curvatures. For the search of possible MBR effects, the calculation procedure introduced in our earlier paper (Mikula *et al.*, 2008b) was used. Figure 3 shows the related azimuth–Bragg angle relationships for the occurrence of the secondary lattice planes (represented by the reciprocal lattice points determined by the vector $g_{2,i}$ on the Ewald sphere) accompanied the primary Si(002) one. The index i means that there could be more than one additional reciprocal lattice points on the Ewald sphere simultaneously. It can be seen from Figure 1(b) that due to the crystal symmetry, it follows that when a secondary

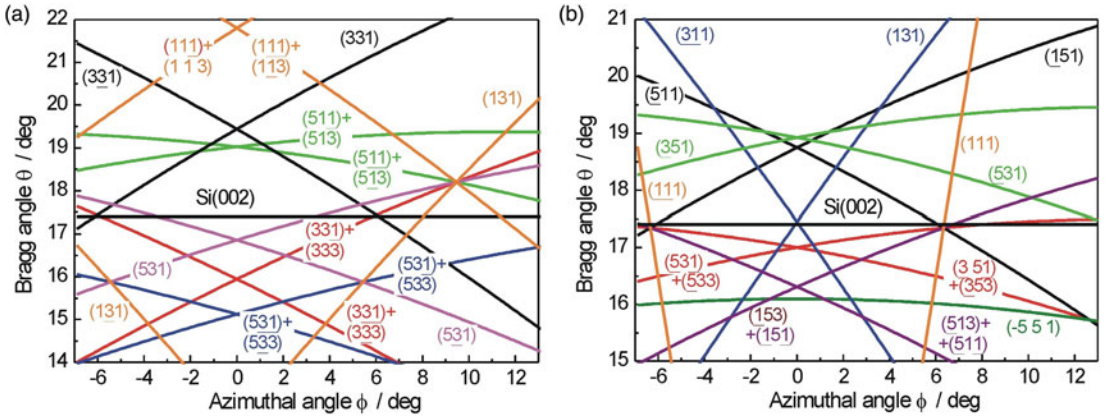

Figure 3. Parts of the azimuth vs. Bragg angle relationship for the 002 primary reflection of the diamond structure as related to the experimental conditions of the slab: (a) the main face is parallel to (100) lattice planes and (b) the main face is parallel to (110) lattice planes.

https://doi.org/10.1017/S0885715620000779 Published online by Cambridge University Press

reflection fulfils the Bragg condition simultaneously with the primary one, there exists automatically the tertiary reflection defined by $g_{3,i} = g_1 - g_{2i}$.

The experiment was carried out on the neutron optics diffractometer NOP (installed at the Řež nuclear reactor LVR-15 – http://www.ujf.cas.cz/en/departments/department-of-neutron-physics/instruments/lvr15/hk8b/) operating at the fixed neutron wavelength of $\lambda = 0.162$ nm provided by the fixed bent-perfect Si(111) pre-monochromator. The Si(002) slabs were situated on the second axis of the diffractometer. The beam incident on the Si(002) slabs was limited to the cross section of 20×10 mm^2 (width × height). For the rotation of the crystal around the scattering vector, a goniometer was used. Due to the construction of the four-point bending device (Mikula *et al.*, 2000) and the goniometer head for the azimuthal rotation, only the range of azimuthal angles ϕ from $-7°$ to $12°$ could be used.

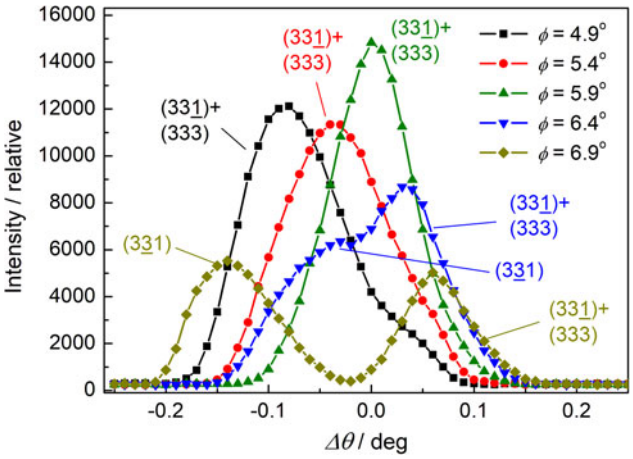

Figure 5. Si(002) rocking curves measured in the vicinity of the mean Bragg angle for several different azimuthal angles and $R = 12$ m.

III. EXPERIMENTAL RESULTS

A. The main face of the crystal slab parallel to the (100) lattice planes

First, the rocking curves of the bent Si(002) crystal with respect to the bent Si(111) pre-monochromator for different individual azimuthal angles ϕ were carried out. Figure 4 shows a 3D map of the MBR effects constructed on the base of the individual rocking curves carried out in the vicinity of the mean Bragg angle. In relation to Figure 3, the rocking curves mean short $\Delta\theta$ scans with respect to the horizontal line (representing the mean Bragg angle $\theta = 17.4°$ which corresponds to the primary reflection) for each azimuthal angle ϕ. Figure 5 demonstrates several rocking curves at different azimuthal angles which show a contribution of some of MBRs. The effect of the MBR phenomenon can be also shown by the ϕ-rotation of the crystal slab for a constant value of the Bragg angle θ. Figure 6 shows the occurrence of the MBR effect as a function of the azimuthal angle ϕ for two values of $\Delta\theta$ from the mean Bragg angle θ. Finally, Figure 7 shows a 2D map of the MBR effects as constructed from the individual rocking curves in the vicinity of the azimuthal angle $\phi = 6°$

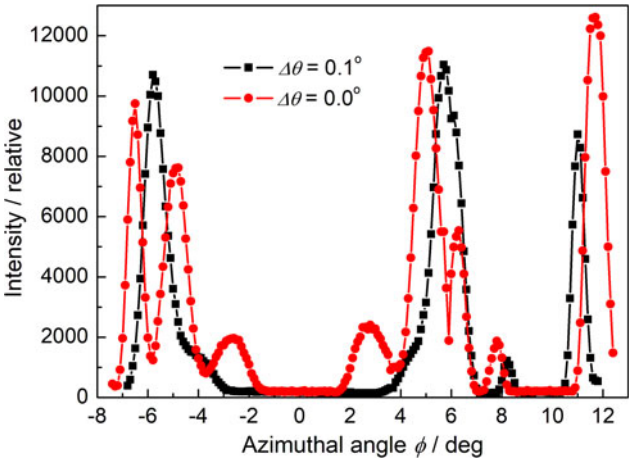

Figure 6. Intensity of the MBR effect vs. the azimuthal angle ϕ for two values of $\Delta\theta$ from the mean Bragg angle.

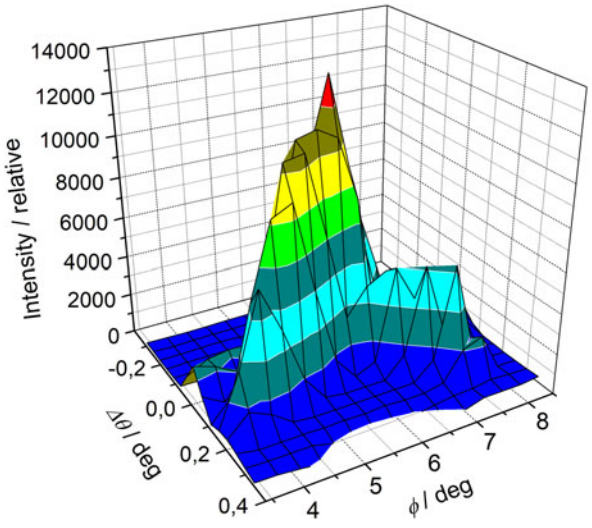

Figure 4. 3D representation of the MBR effects for different azimuthal angles ϕ and the bending radius of the Si(002) slab of $R = 12$ m.

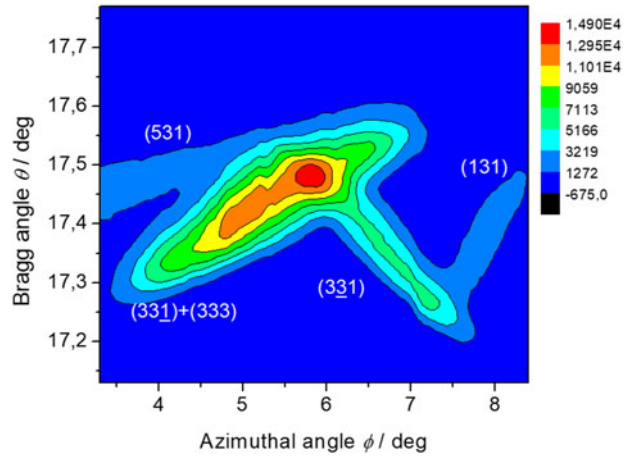

Figure 7. 2D map of the MBR effects constructed at the vicinity of the azimuthal angle $\phi = 6°$.

https://doi.org/10.1017/S0885715620000779 Published online by Cambridge University Press

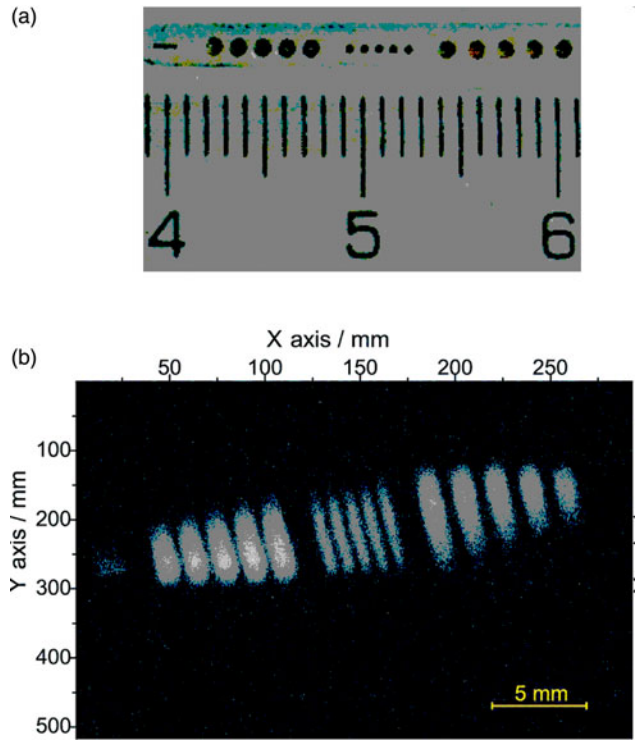

Figure 8. Photo of the holes in a Cd sheet (a) as imaged by IP at a distance of 60 cm from the holes (b).

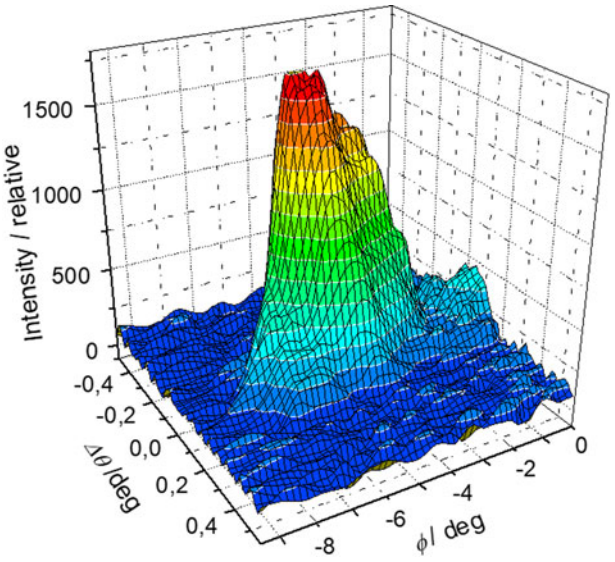

Figure 9. 3D representation of the MBR effects in the vicinity of the mean Bragg angle for different angles ϕ and $R = 9$ m.

in more detail. It should be pointed out that the form of the 2D map follows the lines of MBR occurrences from Figure 3(a). Then, after setting the Si(002) slab at the peak position for $\phi = 5.4°$ (see Figure 5), the divergence of the neutrons obtained by the MBR phenomenon was tested by means of small holes in the Cd sheet inserted into the MBR beam just close to the Si (002) crystal and imaged by imaging plate (IP) at the distance of 60 cm. It can be seen from Figure 8 that the individual images are slightly inclined and perpendicular to the line $(33\underline{1})/(\underline{3}33) + (333)/(\underline{3}3\underline{1})$ from Figure 3(a). The images of the holes confirm that the MBR beam is horizontally (in the scattering plane) highly collimated. An estimation provides the value of about 1.5×10^{-3} rad. However, the beam is vertically poorly collimated as coming from the Si(111) crystal.

B. The main face of the crystal slab parallel to the (110) lattice planes

A similar experiment was also carried out with another cut of the crystal slab, when the main face was parallel to the planes (110). The related 3D representation of the MBR effects based on the rocking curves of the Si(002) planes for different azimuthal angles ϕ and the bending radius of the Si (002) slab of $R = 9$ m is shown in Figure 9. Figure 10(a) shows several rocking curves for different azimuthal angles. On the other hand, Figure 10(b) demonstrates the influence of the degree of crystal deformation on the visibility of the MBR effect. As the rocking curves are not of the Gaussian form, in the next step the diffracted beam was imaged by IP at the distance of 30 cm from the MBR crystal for different ϕ positions (see Figure 11). In relation to possible MBR expectations displayed in Figure 3, it can be decided that the images shown in Figure 11 consist principally of two MBR contributions. The vertical part corresponds to the MBR effect related to the cooperative action of the secondary/tertiary planes $(\underline{1}11)/(111)$, while the inclined part corresponds to the MBR effect related to the two pairs of planes $(\underline{5}13)/(5\underline{1}1) + (\underline{5}1\underline{1})/$

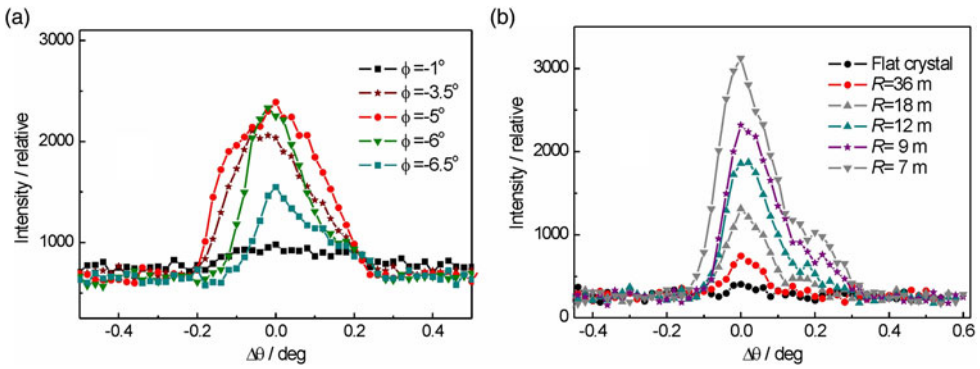

Figure 10. Several rocking curves for (a) different azimuthal angles ϕ at a constant $R = 9$ m and (b) rocking curves for several radii of curvature of the Si slab at the azimuthal angle of $\phi = -6°$.

https://doi.org/10.1017/S0885715620000779 Published online by Cambridge University Press

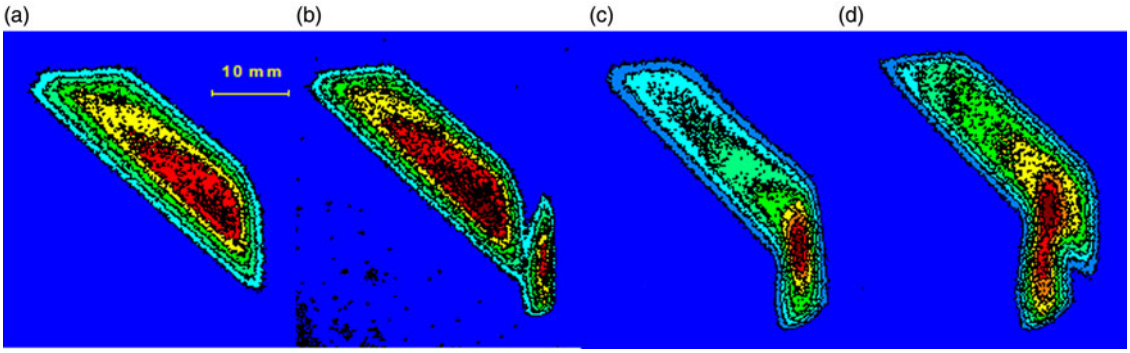

Figure 11. Images of the MBR beam as taken by IP in the peak position of the rocking curve for (a) $\phi = -5°$, (b) $\phi = -5.5°$, (c) $\phi = -6°$, (d) $\phi = -6.5°$, and $R = 7$ m.

(513). In this way, it is necessary to point out that the incident beam from the pre-monochromator has a rather poor collimation (no Soller collimators were used and the width of the incident beam was 20 mm), and therefore, the phase-space element of the incident beam $\Delta\theta \times \Delta\lambda$ is rather large. It brings about that the related MBR effects shown in the rocking curves or their azimuthal dependence are rather broad. It should be pointed out that in the case of images shown in Figure 11, they are not constructed from the rocking curves (see Figures 4, 7, and 9) but taken by IP at chosen individual points given by the coordinates θ and ϕ. The dimensions of the diffracted images depend on the cross-section of the incident beam on the Si(002) slab as well as the vertical divergence of the beam and of course, on the distance of IP from the slab. However, each local place of the image provides a high spatial resolution as has already been demonstrated in the radiography experiment with other MBR monochromatic beam (see, e.g., Mikula *et al.*, 2008b).

IV. SUMMARY

MBRs related to forbidden Si(002) primary reflection and realized in the bent-perfect crystal were investigated in symmetric transmission geometry (with respect to the primary 002 reflection) for two different crystal cuts. As can be seen from Figures 3–7 and 9–11, several strong MBR effects were observed which could be alternatively used for very high-resolution diffraction or transmission experiments. Inclination of the pattern of the monochromatic beam can be avoided by a special cut of the crystal slab having the main face at a suitable chosen ϕ-angle with respect to the 100 or 110 planes. However, not all possible MBR effects which could be expected from Figure 3 were realized and strengthened by the elastic bending. The appearance of the MBR effects and their reflectivity power strongly depend on the mutual orientation of the reciprocal lattice vectors of the secondary and tertiary reflections g_{2i} and g_{3i} with respect to the deformation vector which is in this case of cylindrical bending perpendicular to the g_1 lattice vector of the primary reflection. Moreover, it also depends on the values of Miller indexes h,k,l. For large values of $(h^2 + k^2 + l^2)^{1/2}$, the corresponding Bragg angle increases while the reflectivity power decreases (e.g., for Si(353) reflection planes, the Bragg angle is $\theta = 78°$).

The MBR effect in elastically deformed perfect crystal is realized by the double-diffraction process on pairs of secondary and tertiary lattice planes which are mutually in dispersive setting. Therefore, as expected, the obtained output beam is naturally highly monochromatic and highly collimated (namely in the horizontal plane) without the use of any collimator. However, there are still open questions which should be solved in the search of strong MBR effects, Monte Carlo (MC) simulations of the MBR processes would be desirable. First attempts of MC simulations of an Si(111) primary reflection accompanied by an MBR reflection have been done (Šaroun *et al.*, 2011).

ACKNOWLEDGEMENTS

Measurements were carried out at the CANAM infrastructure of the NPI CAS Řež. The presented results were also supported by the infrastructural MŠMT project LM2018120 (Experimental nuclear reactors LVR-15 and LR-0). P. Mikula acknowledges support from ESS participation of the Czech Republic – OP (CZ.02.1.01/0.0/0.0/16_013/0001794) and J. Šaroun acknowledges support from the project ESS Scandinavia-CZ II (LM2018111). Furthermore V. Ryukhtin acknowledges support from the Czech Academy of Sciences in the frame of the program "Strategie AV21, No. 23". The authors thank Ms. B. Michalcová from NPI CAS for a significant help with the measurements and basic elaboration of the data.

Chang, S. L. (**1984**). *Multiple Diffraction of X-rays in Crystals* (Springer Verlag, Berlin).

Kuich, G. and Rauch, H. (**1965**). "Kohärente Extinktion und Streuung zweiter Ordnung von Neutronen an Einkristallen," Acta Phys. Austriaca **20**, 7–16.

Kuich, G. and Rauch, H. (**1967**). "Intensitätsänderung durch kohärente Extinktion bei Streuung von Neutronen an Einkristallen," Nukleonik **9**, 139–142.

Mikula, P. and Vrána, M. (**2015**). "New type of versatile diffractometer with a double-crystal (DC) monochromator system," Powd. Diffr. **30**(Suppl. S1), S41–S46.

Mikula, P., Vrána, M., and Wagner, V. (**2008b**). "Chapter 5 - Diffraction optics," in *Modern Developments in X-ray and Neutron Optics*, Vol. **137**, edited by A. Erko, M. Idir, T. Krist, and A. G. Michette (Springer, Berlin/Heidelberg), pp. 459–470.

Mikula, P., Vrána, M., Lukáš, P., Šaroun, J., and Wagner, V. (**1996**). "High-resolution neutron powder diffractometry on samples of small dimensions," Mater. Sci. Forum **228–231**, 269–274.

Mikula, P., Kulda, J., Lukáš, P., Vrána, M., Ono, M., and Sawano, J. (**2000**). "Instrumentation components of focusing diffraction used in NPI, ILL, KURRI and PTB," Physica B **276–278**, 174–176.

Mikula, P., Vrána, M., Lott, D., and Wagner, V. (**2006a**). "Neutron monochromator based on dispersive double-reflections excited in a cylindrically bent-perfect-crystal (BPC) slab," Physica B **385–386**, 1274–1276.

Mikula, P., Vrána, M., and Wagner, V. (**2006b**). "Multiple-reflection neutron bent-perfect-crystal (BPC) monochromator," Z. Kristallogr. Suppl. **23**, 205–210.

Mikula, P., Vrána, M., Wagner, V., and Furusaka, M. (**2008a**). "Multiple reflections (MR) – a new challenge for high-resolution neutron diffractometry and spectrometry," Nucl. Instrum. Methods Phys. Res. A **586**, 18–22.

Mikula, P., Vrána, M., Šaroun, J., Seong, B. S., and Em, V. (**2011a**). "Multiple reflections accompanying allowed and forbidden single reflections in bent Si-crystals," Z. Kristallogr. **1**, 169–174.

Mikula, P., Vrána, M., Šaroun, J., Seong, B. S., Em, V., and Moon, M. K. (**2011b**). "Multiple neutron Bragg reflections in single crystals should not be considered negligible," Nucl. Instrum. Methods Phys. Res. A **634**, S108–S111.

Mikula, P., Vrána, M., Šaroun, J., Davydov, V., Em, V., and Seong, B. S. (**2012**). "Experimental studies of dispersive double reflections excited in cylindrically bent perfect-crystal slabs at a constant neutron wavelength," J. Appl. Cryst. **45**, 98–105.

Mikula, P., Vrána, M., Šaroun, J., Krejčí, F., Seong, B. S., Woo, W., and Furusaka, M. (**2013**). "Some properties of the neutron monochromatic beams obtained by multiple Bragg reflections realized in bent perfect single crystals," J. Appl. Cryst. **46**(Part 2), 128–134.

Mikula, P., Vrána, M., Pilch, J., Šaroun, J., Seong, B. S., Woo, W., and Em, V. (**2014a**). "Focusing and reflectivity properties of a parallel double bent crystal (+n,-m) setting," J. Phys.: Conf. Ser. **528**, 012003.

Mikula, P., Vrána, M., Seong, B. S., Woo, W., Em, V., and Korytár, D. (**2014b**). "Neutron diffraction studies of a high resolution double crystal (+n,-m) setting containing Si(220) and Si(311) bent perfect crystals in symmetric and fully asymmetric diffraction geometry, respectively," J. Phys.: Conf. Ser. **528**, 012004.

Mikula, P., Vrána, M., Pilch, J., Seok Seong, B., Woo, W., and Em, V. (**2014c**). "Neutron diffraction studies of double crystal (+n,-m) setting containing a fully asymmetric diffraction geometry (FAD) of a bent perfect crystal (BPC) with the output beam expansion (OBE)," J. Appl. Cryst. **47**(Part 2), 599–605.

Moon, R. and Shull, C. G. (**1964**). "The effects of simultaneous reflections on single-crystal neutron diffraction intensities," Acta Cryst. **17**, 805–812.

Pinsker, Z. G. (**1982**). *X-ray Crystal Optics* (Nauka, Moscow).

Popovici, M. and Yelon, W. B. (**1994**). "Design of microfocusing bent-crystal double monochromators," Nucl. Instrum. Methods Phys. Res. A **338**, 132–135.

Popovici, M. and Yelon, W. B. (**1995**). "Focusing monochromators for neutron diffraction," J. Neutron Res. **3**, 1–25.

Renninger, M. (**1937**). "'Umweganregung', eine bisher unbeachtete Wechselwirkungs-erscheinung bei Raumgitterinterferenzen," Z. Phys. **106**, 141–176.

Renninger, M. (**1960**). "Die verbotenen Reflexe von Diamant, Silicium und Germanium," Z. Kristallogr. **113**, 99–103.

Šaroun, J., Mikula, P., and Kulda, J. (**2011**). "Monte Carlo simulations of parasitic and multiple reflections in elastically bent perfect single-crystals," Nucl. Instrum. Methods Phys. Res. A **634**, S50–S54.

Seong, B. S., Em, V., Mikula, P., Šaroun, J., and Kang, M. H. (**2010**). "Optimization of the bent perfect Si(111) monochromator, at small ($\sim 30^{o}$) take-off angle for stress instrument," J. Appl. Cryst. **43**, 654–658.

Vogt, T., Passell, L., Cheung, S., and Axe, J. D. (**1994**). "Using wafer stacks as neutron monochromators," Nucl. Instrum. Methods Phys. Res. A **338**, 71–77.

Wimpory, R. C., Mikula, P., Šaroun, J., Poeste, T., Li, J., Hoffman, M., and Schneider, R. (**2008**). "Efficiency boost of the materials science diffractometer E3 at BENSC: one order of magnitude due to a double focusing monochromator," Neutron News **19**, 16–19.

Woo, W., Em, V., Seong, B. S., Shin, E., Mikula, P., Joo, J., and Kang, M. H. (**2011**). "Effect of wavelength-dependent attenuation on neutron diffraction stress measurements at depth in steels," J. Appl. Cryst. **44**, 747–754.